J. Braz. Chem. Soc., Vol. 20, No. 5, 873-879, 2009.
Printed in Brazil - ©2009 Sociedade Brasileira de Química
0103 - 5053 $6.00+0.00

Article

Pd-W and Pd-Mo Catalysts for NO Decomposition and NO/CO Reduction Reactions

Rogério M. Dallago[a] and Ione M. Baibich*[*,b]

[a]*Departamento de Química, Universidade Regional Integrada do Alto Uruguai e das Missões, Campus Erechim, Av. Sete de Setembro, 1621, 99700-000 Erechim-RS, Brazil*

[b]*Instituto de Química, Universidade Federal do Rio Grande do Sul, Av. Bento Gonçalves 9500, 91540-970 Porto Alegre-RS, Brazil*

Catalisadores Pd/γ-Al_2O_3 com dois tamanhos de partículas metálicas foram preparados a partir de [Pd(acac)$_2$]. Subsequentemente, a reação fotoquímica de [M(CO)$_6$] (M = Mo ou W) na presença de Pd/γ-Al_2O_3 foi usada para preparar catalisadores bimetálicos Pd-M/γ-Al_2O_3. Os espectros DRIFTS-IVTF das superfícies destes catalisadores antes da decomposição térmica mostraram espécies subcarbonilas [M(CO)$_n$] instáveis. Resultados de quimissorção e adsorção de CO/NO indicaram um bloqueio dos sítios ativos do paládio quando o segundo metal foi incorporado. A atividade catalítica e a seletividade para N_2 e O_2 na reação NO/CO foram maiores para Pd com maior tamanho de partícula, mas foram inibidas quando Mo ou W foram incorporados. Por outro lado, quando esses catalisadores foram testados para a decomposição de NO, a presença de Mo ou W levou a um aumento da atividade catalítica e da seletividade, com os melhores resultados observados na presença de Mo.

Pd/γ-Al_2O_3 catalysts with two different metal particle sizes were prepared from [Pd(acac)$_2$]. Subsequently, the photochemical reaction of [M(CO)$_6$] (M = Mo or W) in the presence of Pd/γ-Al_2O_3 was used to prepare bimetallic Pd-M/γ-Al_2O_3 catalysts. DRIFTS FTIR spectra of the catalyst surfaces prior to thermal decomposition showed unstable subcarbonyl [M(CO)$_n$] species. Chemisorption and CO/NO adsorption results indicated a blockage of the Pd active sites when the second metal was incorporated. The catalytic activity and the selectivity for the NO/CO reaction were higher for Pd with higher particle size, but they were both inhibited when Mo or W were incorporated. On the other hand, when the catalysts were tested for NO decomposition, the presence of Mo or W led to an increase in the catalytic activity, with optimal results observed in the presence of Mo.

Keywords: NO decomposition, NO/CO reduction, palladium/alumina catalyst, molybdenum, tungsten

Introduction

The removal of NO_x species is among the most relevant issues in environmental chemistry.[1,2] Since NO is thermodynamically unstable relative to N_2 and O_2 at low temperatures, the catalytic decomposition of NO to give these two elements presents a simple and attractive method for removal.[2] To this end, a number of metals and inorganic supports have been developed.[3,4]

There has been a growing interest in the use of palladium as the active metal for exhaust catalysts. Studies have shown that Pd can catalyze the reduction of NO to N_2, in addition to its activity for hydrocarbon and CO oxidation.[5-11] However, in the presence of hydrocarbons, the NO reducing capacity of Pd is lower than that reported for Rh-based catalysts.[8,12] In order to overcome this problem while employing relatively inexpensive metals, bimetallic Pd-Mo and Pd-W catalysts have been proposed.[13-21] Using inorganic salt precursors, catalysts with adequate metal-metal contacts can be prepared and employed, but they require the use of high catalyst loadings, which might lead to tungsten or molybdenum oxide vapors.[17]

Previously, we have shown that Pd-M/γ-Al_2O_3 (M = Mo or W) prepared from the photochemical activation of the organometallic precursor [M(CO)$_6$] displayed Pd-M interactions with low metal loadings and led to an enhanced activity for NO decomposition with M = W.[22-26] Furthermore, we have studied different solid supports, such as zeolites[27,28] and mesoporous materials.[29-31]

*e-mail: ione@iq.ufrgs.br

Herein, we describe the preparation of the bimetallic catalysts Pd-Mo/γ-Al_2O_3 and Pd-W/γ-Al_2O_3 from the photochemical activation of [$M(CO)_6$] (M = Mo and W) on alumina, and we investigate the influence of the metal particle size and of the presence of a second metal on the catalysts performance. The catalysts obtained by this method were characterized by Fourier-transform infrared spectroscopy (FTIR) analysis of adsorbed CO and NO, H_2 chemisorption, and metal content determination by atomic absorption spectroscopy (AAS). The activities of the catalysts were investigated for NO + CO and NO decomposition reactions.

Experimental

Catalyst synthesis

Alumina (γ-Al_2O_3, 96 $m^2\ g^{-1}$, Rhône-Poulenc) was activated at 973 K for three hours in synthetic air, followed by 1 h in vacuum at the same temperature.

The palladium on alumina catalyst (Pd/γ-Al_2O_3) was prepared by the wet impregnation technique using a toluene solution of palladium acetylacetonate ([$Pd(acac)_2$], Aldrich, 2.2 mg mL^{-1}) and activated alumina, left in contact for 24 h at room temperature. After impregnation, the liquid was removed, and the solid was activated in air at 573 K for 2 h and then reduced in flowing hydrogen at the same temperature for 2 h, as previously detailed.[22,23] This catalyst was named Pd/γ-Al_2O_3. A certain amount of this catalyst was subjected to a sintering process by further reduction with H_2 for 10 h at 773 K, producing the desired Pd_{sint}/γ-Al_2O_3 catalyst.

The bimetallic Pd-Mo and Pd-W catalysts were prepared using palladium-alumina as support and performing a photochemical activation of [$M(CO)_6$], where M = Mo or W. This was accomplished by adding 2 g of Pd/γ-Al_2O_3 to a degassed and dried hexane solution of the metal carbonyl compound (77 mg [$W(CO)_6$] and 83 mg [$Mo(CO)_6$]) aiming to achieve 2 wt% metal**,** under N_2, using Schlenk techniques. The closed reaction vessel was irradiated for 6 h with a UV Hg lamp fitted into a cold finger. FTIR analysis of the solution and DRIFTS (Diffuse Reflectance Infrared Fourier Transform Spectroscopy) analysis of the support were subsequently carried out. The solid was then separated by filtration, dried under vacuum at 723 K and stored under argon. The percent content of Pd, W and Mo was determined by AAS.

DRIFTS FTIR spectra

Diffuse Reflectance (DRIFTS) spectra were recorded at 293 K on a Bomem MB-102 spectrometer, with 32 scans and a resolution of 4 cm^{-1}. The study was restricted to the ν(CO) region (2200-1700 cm^{-1}). The solid phases were analyzed as powders in a DRIFTS accessory equipped with sampling cups. These were filled with the support powder and transferred immediately to the equipment to prevent decomposition. The spectra were collected in reflectance units and transformed to Kubelka-Munk (KM) units.

Hydrogen chemisorption

Hydrogen chemisorption measurements were made in conventional volumetric equipment at 298 K, employing pulses with varying H_2 pressures (between 60 and 270 torr). The samples were initially treated with H_2 at 573 K for 1 h, followed by vacuum for 18 to 20 h, and by cooling under vacuum to 298 K. The amount of absorbed hydrogen forming α and β palladium hydrides was measured after vacuum at room temperature and subtracted. The dispersion values or the exposed palladium ratio (Pds/Pd) were determined from the difference between the two relevant isotherms (the first one gives the total adsorbed and absorbed amount of hydrogen, while the second measures only the absorbed H_2) that corresponds only to strongly chemisorbed hydrogen (H_{irrev}) and extrapolated to zero pressure, assuming H_{irrev}:metal proportion of 1:1. The crystallite size based on chemisorption measurements was estimated from the equation:[32] d (nm) = 1.12 (percentage of exposed metal)$^{-1}$. This expression assumes hemispherical particles and a surface atom density of 1.27 x 10^{19} atom m^{-2}.

CO and NO adsorption measurements

A Nicolet 20 DXB FTIR instrument at 4 cm^{-1} resolution was used to identify the CO species adsorbed on the catalysts surfaces. Catalyst samples of approximately 30 mg were pressed to form transparent 10 mm diameter disks, which were placed in a heated metal holder. The holder was placed in the beam path of a stainless steel cell sealed with CaF_2 windows, and coupled to a vacuum system for evacuation to 10^{-6} torr. It was possible to perform heat treatments up to 573 K, to dose CO or NO through a leak valve, or to maintain a steady flow of H_2 or He. An MKS Baratron Type 170 M allowed pressure measurements to be made in the 0.1-10 torr range.

After reduction in flowing H_2 at 573 K, the samples were cooled to room temperature under a steady stream of He. The adsorbate was dosed at pressures of 1 to 5 torr, and the samples were exposed to CO or NO prior to spectra measurement. Scanning times were approximately 1 min. Finally, the cell was evacuated to 10^{-5} torr for 2 min, and a new spectrum was accumulated.

Catalytic activity measurements

Catalytic experiments were carried out in a flow reactor mounted in an electric furnace. Catalysts samples (0.3 g for the NO reaction and 0.022 g for the NO + CO reaction) were packed in a 0.6 mm internal diameter stainless steel (SS) tube with a thermocouple placed at the reactor entrance. The NO decomposition reactions were studied as a function of time at 723 K, 753 K and 773 K using a mixture containing 370 ppm of NO in a He background (Matheson, certified), and the flow rate was adjusted to 75 mL min^{-1}. Prior to reaction, the catalysts were reduced *in situ* with H_2 for 45 min at the reaction temperature.

The NO + CO reactions were studied as a function of temperature. The catalyst was treated with the reaction mixture (550 ppm of NO and 550 ppm of CO in He) for 35 min at 673 K prior to all measurements. The flow rate was adjusted to 140 mL min^{-1}. Gas chromatographic separation of reactants and products was achieved by two Porapak Q columns: the first (1/8 in. x 6 m) was employed for the separation of NO, O_2 and N_2 at 263 K, and the second (1/8 in. x 2.4 m) was employed for the separation of N_2O and CO_2 at 313 K.

Results and Discussion

Adsorbed metal carbonyl FTIR spectra

DRIFTS spectral analysis of solid samples immediately after the photochemical reaction and prior to thermal decomposition indicated the $[M(CO)_{6-n}]$ (n = 1-6) uptake on the support, as shown in Figure 1. The spectrum was recorded in inert atmosphere to allow the detection of the bands, since these species decompose rapidly in the absence of a stabilizing ligand such as PPh_3.[25,26]

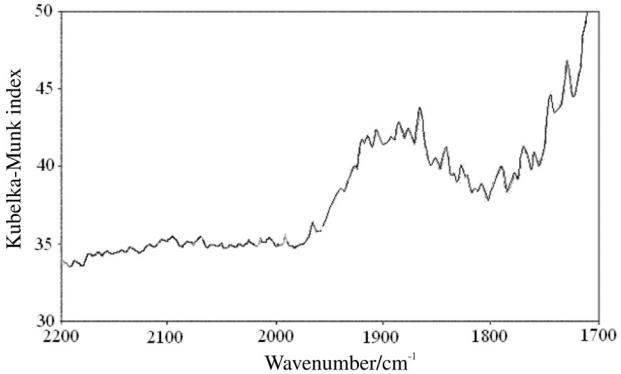

Figure 1. DRIFTS IR spectrum in the ν(CO) region of Pd_{sint}/γ-Al_2O_3 after 6 h reaction.

The photochemical activation was monitored by measurement of the decrease in the $[M(CO)_6]$ t_{1u} mode of the ν(CO) stretching band in the hexane solution spectrum. When the support was Pd_{sint}/γ-Al_2O_3, the solution displayed bands at 2078 and 1948 cm^{-1} at the zero time point (Figure 2a). This was in direct contrast to the Pd/γ-Al_2O_3 support spectrum, in which the Pd was not submitted to high temperature reduction, even after 6 h. In this case, the metal hexacarbonyl band remained unchanged (Figure 2b). The bands shown in Figure 2a are indicative of an $[M(CO)_5]$ species shifted to higher wavenumbers relative to $[M(CO)_5PPh_3]$, where the phosphine ligand acts as a Lewis base. The larger Pd particles were determined to be reactive toward CO, and even prior to photochemical activation, the tungsten hexacarbonyl loses one CO that likely coordinates to Pd.

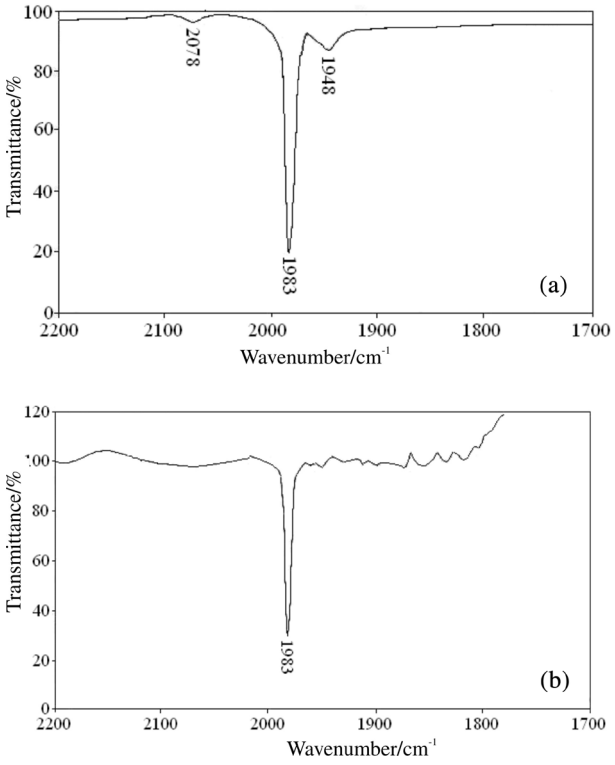

Figure 2. Spectra of $[W(CO)_6]$ in hexane solution (a) after immediate contact with Pd_{sint}/γ-Al_2O_3; (b) after 6 h contact with Pd/γ-Al_2O_3.

Catalysts characterization

Table 1 presents catalyst loadings, dispersions, and particle sizes determined for the present study. It is evident that the Pd_{sint}/γ-Al_2O_3 catalyst presents a reduction in the dispersion and a subsequent increase in particle size relative to Pd/γ-Al_2O_3. The high-temperature reduction led to a pronounced particle agglomeration. There is also a decrease in Pd H_2 adsorption caused by Mo or W in the bimetallic catalysts. This effect can be attributed to a blockage of the palladium-exposed surface by the second metal, preventing

two adjacent Pd atoms to adsorb H_2. Similar results were reported by Schmal *et al.*[16] for Pd-MoO_3/alumina catalysts prepared from inorganic salts.

Table 1. Catalysts loadings and hydrogen chemisorption

Catalysts	%Metal			Dispersion	dp/nm
	Pd	W	Mo	Pd_S/Pd_T	Chem.H_2[a]
Pd	0.87	-	-	0.66	1.7
Pd_{sint}	0.87	-	-	0.40	2.8
Pd_{sint}Mo	0.87	-	1.0	0.28	-
Pd_{sint}W	0.87	0.66	-	0.24	-

[a]Assuming semispherical particles: dp = 1.12 $(Pd_S/Pd_T)^{-1}$.

CO and NO adsorption measurements

Figure 3 shows the FTIR spectra of the ν(CO) region for the two catalysts after 5 min CO exposure and subsequent 2 min under vacuum. The bands are typical for CO adsorbed on Pd. The band at higher wavenumber (*ca.* 2075 cm^{-1}) is attributed to linear CO, and the bands at 1958 and 1908 cm^{-1} are attributed to bridging CO. There is a clear lowering of the linear CO band intensity and a concomitant increase in the bridging CO band with the sintering process. This is in accordance with the results shown in Table 1, which suggest that the larger Pd particles present shorter Pd atom distances and a higher probability for CO to bind in a bridging manner. Additionally, the weak band at 2110 cm^{-1}, which disappears in Pd_{sint}/γ-Al_2O_3, is attributed to Pd^+ species.

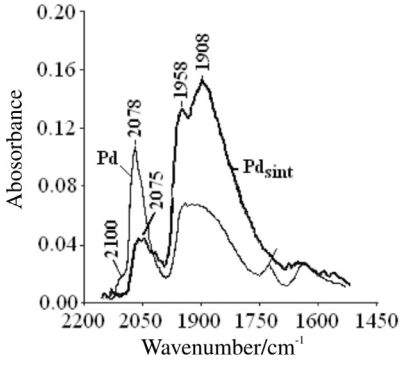

Figure 3. FTIR spectra of the ν(CO) region of Pd/γ-Al_2O_3 and Pd_{sint}/γ-Al_2O_3 catalysts after 5 min CO exposure followed by 2 min under vacuum.

The effect of the second metal atom in the sintered bimetallic catalysts was to lower both the bridging and the linear CO band intensities (Figure 4). It is well known that Mo and W adsorb CO only under extremely harsh conditions (> 873 K), and in the present case the band shapes are similar to those in Figure 3. As such, it can be assumed that they are due to CO adsorbed on Pd.[32-36] The same behavior was previously observed with the Pd-W/Al_2O_3 catalyst.[25] Additionally, there is a decrease in the probability of having two adjacent Pd atoms binding CO in a bridging manner. An electronic effect caused by the presence of Mo or W was not detected, since there is not a significant shift in the ν(CO) bands.

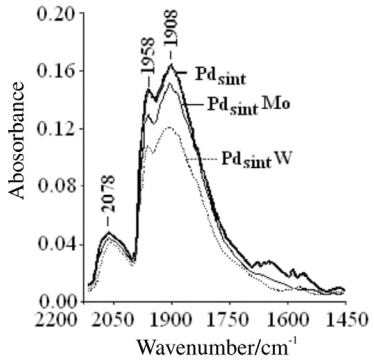

Figure 4. FTIR spectra of the ν(CO) region of Pd_{sint}/γ-Al_2O_3 , Pd_{sint} - Mo/γ-Al_2O_3 , Pd_{sint} - W/γ-Al_2O_3 catalysts after 5 min CO exposure followed by 2 min under vacuum.

The spectra of the ν(NO) region for the Pd_{sint} catalysts after NO exposure are shown in Figure 5. The band near 1730 cm^{-1} is attributed to ν(NO) terminal stretching band, and the band at 1626 cm^{-1} is assigned to bridging NO. The bands that appear at lower wavenumbers might be attributed to multi-coordinated NO or, as reported before,[25] to carbonates from a possibly contaminated surface, as CO adsorption was measured before the measurements with NO. There is a decrease in band intensity in the presence of the second metal (Mo or W), with this effect being higher for W. This is in accordance with the results found for CO adsorption described above.

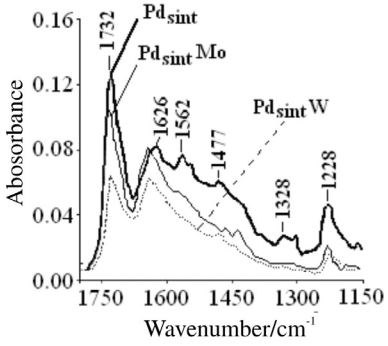

Figure 5. FTIR spectra of the ν(NO) region of Pd_{sint}/γ-Al_2O_3, Pd_{sint}-Mo/γ-Al_2O_3 , Pd_{sint}-W/γ-Al_2O_3 catalysts after 5 min NO exposure followed by 2 min under vacuum.

Catalytic activities results

The prepared catalysts were tested for the NO + CO reduction reaction as a function of temperature. Figure 6 shows the monometallic Pd catalyst behavior. The results

indicate that the larger particle size catalyst presented slightly higher activities to both CO oxidation and NO reduction. Furthermore, higher selectivities toward N_2 and lower selectivities toward N_2O were observed in temperatures above 573 K. The proximity of the Pd active site appears to explain this higher activity. Using the NO conversion values at 523 K (Figure 6), the number of molecules that were converted *per* second calculated from the reaction conditions (experimental part) and the hydrogen chemisorption values reported in Table 1, which allow the estimation of the number of Pd atoms, the turnover frequency (TOF_{NO}) was estimated to be 14.48×10^{-3} for Pd/γ-Al_2O_3 and 35.84×10^{-3} for Pd_{sint}/γ-Al_2O_3. On the other hand, the presence of Mo or W on the Pd_{sint} catalyst (Figure 7) did not significantly decrease the activity for NO reduction; rather, it inhibited CO oxidation and N_2 production and increased the overall N_2O concentration. These results suggest that the presence of W or Mo did not improve the reaction performance in the presence of CO.

Figure 8 illustrates the NO conversion values *versus* time at 773 K for the NO decomposition reaction using Pd_{sint}/γ-Al_2O_3 catalysts. After 10 min, the catalysts were nearly completely deactivated. Production of N_2O was not detected using the monometallic Pd catalyst, which indicates complete NO reduction. When the second metal was W, only traces of N_2O were observed (< 1 ppm), and the O_2 production was high (10 to 15 ppm), indicating nearly complete NO reduction. The Pd_{sint}-Mo catalyst presented a different behavior, in which high conversion and residual activities higher than for Pd_{sint} and Pd_{sint}-W catalysts were observed for extended periods of time. Furthermore, the starting point of N_2O production coincides with a decrease in total NO conversion after 10 min. Analogous behavior was also observed in the Pd/γ-Al_2O_3 based catalysts with

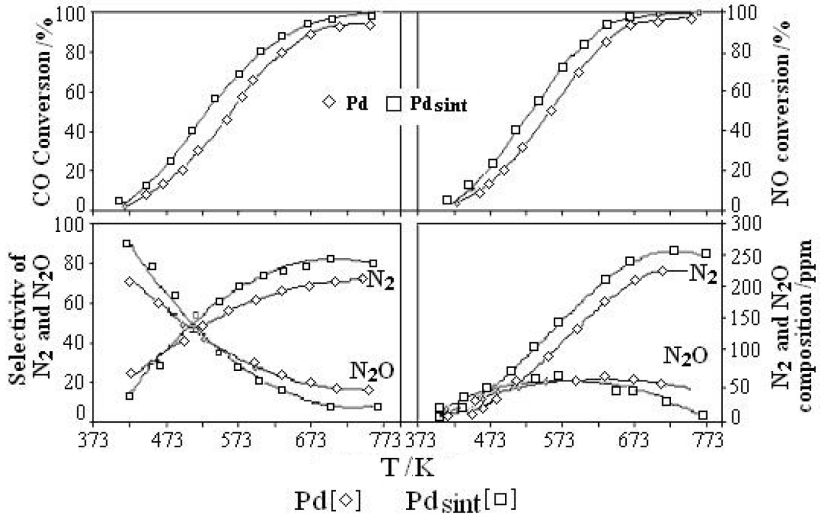

Figure 6. Conversion *versus* temperature and selectivity in the NO + CO reactions. Catalysts are Pd/γ-Al_2O_3 and Pd_{sint}/γ-Al_2O_3.

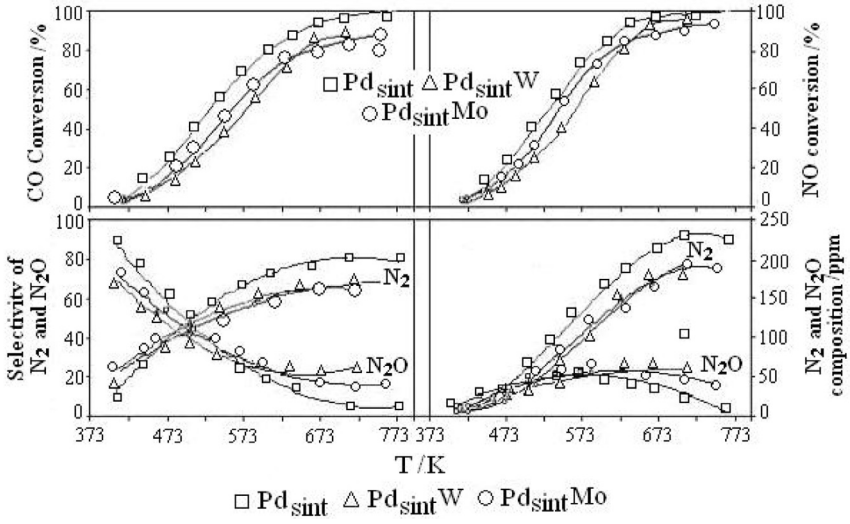

Figure 7. Conversion *versus* temperature and selectivity in the NO + CO reaction. Catalysts are Pd_{sint}, Pd_{sint}W and Pd_{sint}Mo.

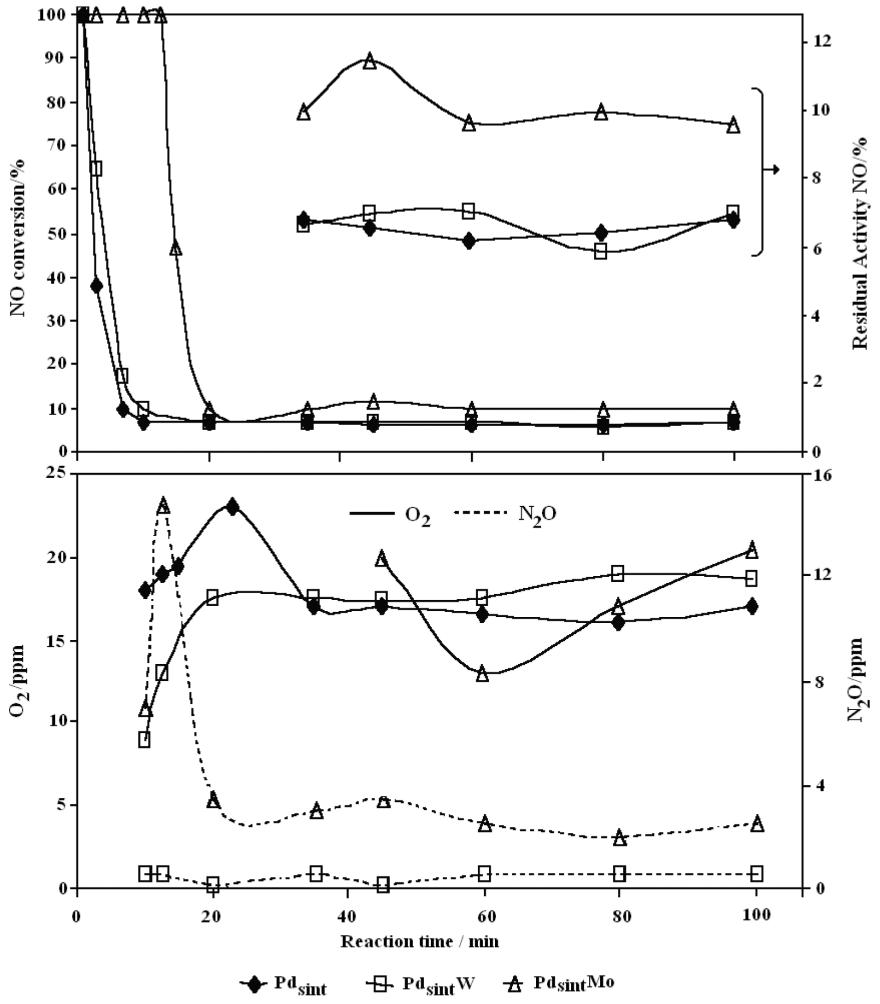

Figure 8. Activity evolution (a) and O_2 and N_2O formation (b) for Pd_{sint} catalysts at 773 K in the NO decomposition reaction.

smaller size particles (data not shown). Table 2 shows the activation energies found for these catalysts in the temperature range between 723 and 773 K. It is evident that the presence of Mo results in a significant decrease in the activation energy for the NO reduction reaction.

Table 2. Activation energy values for NO reduction

Catalyst	%metal			E_a / (kcal mol^{-1})
	Pd	W	Mo	
Pd_{sint}	0.87	-	-	22.31
$Pd_{sint}W$	0.87	0.66	-	19.63
$Pd_{sint}Mo$	0.87		1.0	8.35

The IR CO and NO bands (Figures 4 and 5) were not shifted when W or Mo were present, and therefore changes in the surface electronic properties of Pd were not detected. As Mo does not block the Pd active sites, differently from W, even being in higher loadings, the promotional effect of Mo can be attributed to adsorption and dissociation of NO on partially reduced Mo atoms. This effect is in accordance with the results reported by Schmal *et al.*[34] comparing activities and selectivities of Pd and Pd-MoO_3 catalysts. The authors found that both catalysts gave the same conversion, although the fraction of exposed metal atoms decreased substantially in the presence of 7.5% Mo. In our case, where Mo is in a low oxidation state (as the catalyst precursor contained Mo^0), the effect is accentuated in accordance with the results found. Finally, in comparison with W, the better result for Mo may be related to the lower reduction temperature of Mo.

Conclusions

It has been demonstrated that Pd particles with larger sizes are more active and selective towards the NO + CO reduction reaction. The photochemical activation of metal carbonyls provided synthetic access to bimetallic Pd-Mo and Pd-W catalysts. The activities and selectivities of these bimetallic catalysts were lowered by the presence of W or

Mo in the NO reduction by CO. However, these bimetallic catalysts were more active and selective in the direct NO decomposition reaction, with optimal results observed for the Mo-containing catalyst.

Acknowledgments

This work was supported by CNPq, FAPERGS and CAPES (Brazil). We are grateful to Carlos Gigola, PLAPIQUI, Bahia Blanca, Argentina, for the use of his laboratory facilities.

References

1. Liu, Z.; Woo, S. I.; *Catal. Rev.* **2006**, *48*, 43.
2. Fritz, A.; Pitchon, V.; *Appl. Catal., B* **1997**, *13*, 1.
3. Taylor, K. C.; *Appl. Catal., B* **1993**, *35*, 457.
4. Summers, J. C.; Monroe, D. R.; *Ind. Eng. Chem. Prod. Res. Dev.* **1981**, *20*, 23.
5. Burch, R.; Ramli, A.; *Appl. Catal., B* **1998**, *15*, 49.
6. Obuchi, A.; Ohi, A.; Nakamura, M.; Ogata, A.; Mizuno, K.; Ohuchi, H.; *Appl. Catal., B* **1993**, *2*, 71.
7. Hecker, W. C.; Bell, A. T.; *J. Catal.* **1983**, *84*, 200.
8. Muraki, H.; Shinjoh, H.; Fujitani, Y.; *Ind. Eng. Chem. Prod. Res. Dev.* **1986**, *25*, 419.
9. Pieterse, J. A. Z.; Booneveld, S.; *Appl. Catal., B* **2007**, *73*, 327.
10. Granger, P.; Dujardin, C.; Paul, J. F.; Leclerq, G.; *J. Mol. Catal. A: Chem.* **2005**, *228*, 241.
11. Granger, P.; Dhainaut, F.; Pietrzik, S.; Malfoy, P.; Mamede, A.S.; Leclerq, L.; Leclerq, G.; *Top. Catal.* **2006**, *39*, 65.
12. Shelef, M.; Graham, G. W.; *Catal. Rev. - Sci. Eng.* **1994**, *36*, 433.
13. Halasz, I.; Brenner, A.; Shelef, M.; *Catal. Lett.* **1992**, *16*, 311.
14. Halasz, I.; Brenner, A.; Shelef, M.; *Catal. Lett.* **1993**, *18*, 289.
15. Halasz, I.; Brenner, A.; Shelef, M.; *Appl. Catal., B* **1993**, *2*, 131.
16. Schmal, M.; Baldanza, M. A. S.; Vannice, M. A.; *J. Catal.* **1999**, *185*, 138.
17. Damiani, D. E.; Juan, A.; Konopny, L. W.; *Appl. Catal., B* **1998**, *15*, 115.
18. Maire, G.; Hilaire, L.; Bigey, C.; *J. Catal.* **1999**, *184*, 406.
19. Leclercq, G.; El Gharbi, A.; Gengembre, L.; Romero, T.; Pietrzyk, S.; Leclercq, L.; *J. Catal.* **1994**, *148*, 550.
20. Wolf, E. E.; Fleisch, T. H.; Regalbuto, J. R.; *J. Catal.* **1987**, *107*, 114.
21. Wolf, E. E.; Allen, C. W.; Regalbuto, J. R.; *J. Catal.* **1987**, *108*, 304.
22. Baibich, I. M.; dos Santos, J. H. Z.; Stedile, F. C.; Baumvol, I. J. R.; Santarosa, V. E.; *Phys. Status Solid B* **1995**, *192*, 519.
23. Baibich, I. M.; dos Santos, J. H. Z.; Stedile, F. C.; Baumvol, I. J. R.; Santarosa, V. E.; *Polyhedron* **1997**, *16*, 1937.
24. Baibich, I. M.; dos Santos, J. H. Z.; Gigola, C.; Sica, A. M.; da Silveira, V. C.; *Can. J. Anal. Sci. Spectrosc.* **1998**, *43,* 26.
25. Baibich, I. M.; dos Santos, J. H. Z.; Gigola, C.; Sica, A. M.; *J. Mol. Catal. A: Chem.* **1999**, *137*, 287.
26. Sica, A. M.; Baibich, I. M.; Gigola, C. E.; *J. Mol. Catal. A: Chem.* **2003**, *195*, 225
27. de Oliveira, A. M.; Crize, L. E.; da Silveira, R. S.; Pergher, S. B. C.; Baibich, I. M.; *Catal. Commun.* **2007**, *8*, 1293.
28. de Oliveira, A. M.; Baibich, I. M.; Machado, N. R. C. F.; Mignoni, M. L.; Pergher, S. B. C.; *Catal. Today* **2008**, *133*, 560.
29. Cónsul, J. M. D.; Peralta, C. A.; Benvenutti, E. V.; Ruiz, J. A. C.; Pastore, H. O.; Baibich, I. M.; *J. Mol. Catal. A: Chem.* **2006**, *246*, 33.
30. Cónsul, J. M. D.; Peralta, C. A.; Ruiz, J. A. C.; Pastore, H. O.; Baibich, I. M.; *Catal. Today* **2008**, *133*, 475.
31. Cónsul, J. M. D.; Costilla, I.; Gigola, C. E.; Baibich, I. M.; *Appl. Catal. A: Gen.* **2008**, *339*, 151.
32. Anderson, J.; *Structure of Metallic Catalysts*, Academic Press: New York, 1975, p. 296.
33. Topsöe, N. -Y.; Topsöe, H.; *J. Catal.* **1982**, *75*, 354.
34. Schmal, M.; Noronha, F. B.; Baldanza, M. A. S.; *J. Catal.* **1999**, *188*, 270.
35. Xin, Q.; Yan, Y.; Jiang, S.; Guo, X.; *J. Catal.* **1991**, *131*, 234.
36. Zecchina, A.; Garrone, E.; Ghiotti, G.; Coluccia, S.*; J. Phys. Chem.* **1975**, *79*, 972.

Received: September 30, 2008
Web Release Date: March 27, 2009